ELSEVIER

Polymer 40 (1999) 2077–2084

polymer

Influence of glass bead fillers on phase transitions of syndiotactic polypropene

F. Stricker, R.-D. Maier, M. Bruch, R. Thomann, R. Mülhaupt*

Freiburger Materialforschungszentrum und Institut für Makromolekulare Chemie der Albert-Ludwigs-Universität, Stefan-Meier-Straße 21, D-79104 Freiburg, Germany

Received 22 December 1997; revised 5 March 1998; accepted 17 March 1998

Abstract

The influence of glass beads on the phase transition of syndiotactic polypropene has been investigated. The glass transition at 4°C, detected by means of dynamic mechanical analysis, and multiple melt behaviour, detected by means of differential scanning calorimetry (DSC), does not depend upon the presence of glass bead fillers. However, dynamic mechanical analysis shows an unexpected phase transition at 55°C. This transition, which is not found for neat syndiotactic polypropene, can be also detected by DSC and pressure–volume–temperature (PVT) measurements. The signal detected by PVT appears at higher temperatures, due to higher pressure during measurement. Wide angle X-ray scattering (WAXS) measurements reveal that neat syndiotactic polypropene crystallizes in unit cell II, whereas glass bead-filled syndiotactic polypropene crystallizes in unit cells I and II. Glass bead-filled syndiotactic polypropene, heated up above 60°C, shows a WAXS pattern corresponding to unit cell II. From these results, it can be concluded, that glass beads can nucleate the formation of unit cell type I, which transforms into unit cell type II upon heating at 55°C.

Keywords: Syndiotactic polypropylene; Phase transition; Dynamic mechanical analysis

1. Introduction

The crystallization behaviour, structure and morphology of unfilled syndiotactic polypropylene (s-PP) are already well investigated [1–6]. Early investigations used s-PP of poor stereoregularity and low molecular weight. In 1988, Ewen discovered that stereorigid metallocenes, combined with methylaluminoxane, catalyse propene polymerization to afford highly stereotactic s-PP [7]. This development has generated renewed scientific interest in the crystallization behaviour and morphology of s-PP. Three different chain conformations have been observed, a planar zigzag chain with $(tttt)_n$-conformation [8–11], that converts to a $(t_6g_2t_2g_2)_n$ conformation upon exposure to benzene, toluene or *p*-xylene below 50°C for several days [12]. Crystal structures that are based on these helical conformations transform upon heating to stable crystalline structures consisting of helices with a $(ttgg)_n$ conformation (s(2/1)2) [11]. Based on the $(ttgg)_n$ conformation three orthorhombic crystal modifications, types I, II, and III, have been observed [6, 13–15]: type I, with a c-centered unit cell composed of helices of one hand only [13], type II with a face-centered unit cell on the ac plane, space group $Pca2_1$, and alternating handedness of the helices along the *a*-axis, and finally type III with antichiral packing of the helices along the *a*- and *b*-axes, space group Ibca [6, 14, 15]. Upon heating, type I transforms to type II or III [11]. s-PP shows multiple melting behaviour, especially at lower isothermal crystallization temperatures. Marigo et al. [16] associated the low temperature transition of the DSC heating curve with structures formed at the crystallization temperature, while the high temperature endotherm corresponds to crystal reorganization during scanning. The reorganization is accompanied by the appearance of a strong 221 cell type III reflection in WAXS experiments [2, 3]. The objective of this research is to investigate the influence of glass bead fillers on phase transitions of s-PP. As shown in previous work, glass beads can nucleate s-PP crystallization [17]. Dynamic-mechanical analysis (DMA) of glass bead-filled s-PP showed an unexpected phase transition at about 54°C. Aminopropyl-functionalized glass beads of 5 μm average diameter were blended together with s-PP in a twin-screw blender with counter-rotating screws at 60 rpm and 200°C. The thermal phase behaviour was examined by dynamic mechanical analysis (DMA), differential scanning calorimetry (DSC),

* Corresponding author..

0032-3861/99/$ - see front matter
PII: S0032-3861(98)00247-X

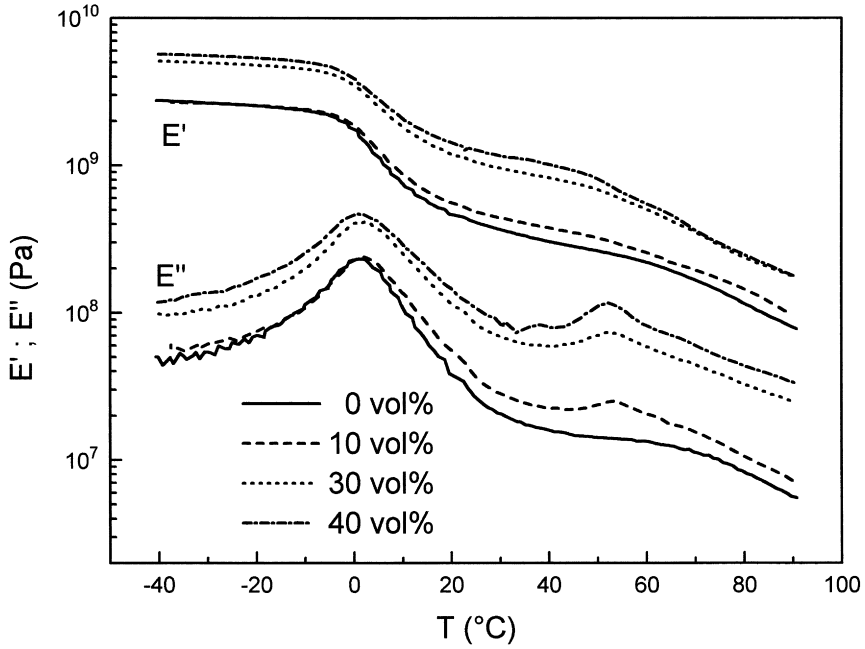

Fig. 1. Influence of temperature on the dynamic mechanical storage and loss modulus, E' and E'', of s-PP containing different glass bead volume fraction ϕ_f.

pressure–volume–temperature (PVT) measurements and wide angle X-ray scattering (WAXS).

2. Experimental

2.1. Materials

Syndiotactic polypropene (s-PP; SPH-40; $M_n = 80\ 000$ g/mol; $M_w/M_n = 1.7$; racemic triades, determined by ^{13}C n.m.r. = 91.1%; MFI = 3.5 g/10 min at 230°C), supplied by Mitsui, was used without further purification. Aminopropyl-functional glass beads (Potters-Ballotini 5000 CP-03, average diameter of 5 μm, 97% smaller than 12 μm), containing a 0.02 wt% coating of aminopropyltrimethoxysilane, were used as a filler component. 0.2 wt% Irganox 1010/Irgafos 168 (4/1 wt.%) were added as a stabilizer during melt processing.

2.2. Composite preparation

All composites were prepared under identical mixing and moulding conditions. Filler volume fractions were varied between 0 and 40 vol%. Melt blending was performed in a Haake Rheomix 90 twin-screw kneader equipped with a 60 ml mixing chamber that was preheated at 200°C. Typically s-PP was molten together with the stabilizers for 1.5 min. Then the filler was added. After 4 min total mixing time the sample was quickly recovered and quenched between metal plates. Sheets of 2 mm thickness were prepared by compression moulding in an evacuated press (Schwabenthan Polystat 100), annealing at 210°C for 10 min and quenching to room temperature between water-cooled metal plates. Rectangular bars of a dimension of $10 \times 6 \times 2$ mm were cut out of these plates for evaluation of dynamic mechanical properties.

2.3. Dynamic mechanical analysis

Dynamic mechanical measurements were carried out with the aid of a Rheometrics Solid Analyser RSA II and dual-cantilever geometry (frequency 1 Hz; heating rate 2 K/min). The temperature range was − 40 to 100°C. Prior to measurement the samples were dried at 60°C in vacuum for 12 h. This garantees uniform humidity of the samples.

2.4. PVT measurements

The specific volumes of neat and filled s-PP samples were determined by means of a Micropynometer (Quantachrome) and monitored as a function of pressure and temperature using a Gnomix PVT apparatus [18]. The sample cell was filled with approximately 1 cm^3 of the sample and mercury. Measurements were performed in the isobaric mode. The specific volume of the sample was recorded at a pressure of 10 MPa in the temperature range between 40 and 180°C with a heating rate of 2 K/min.

2.5. DSC measurements

Melting temperatures were recorded on a Perkin-Elmer DSC-7 using a heating rate of 2 K/min. Prior to measurement, the samples were heated at 60°C for 12 h.

2.6. WAXS

The WAXS measurements were carried out with a Siemens D500 apparatus. For the measurements a CuK_a radiation of a wavelength $l = 0.154$ nm was used.

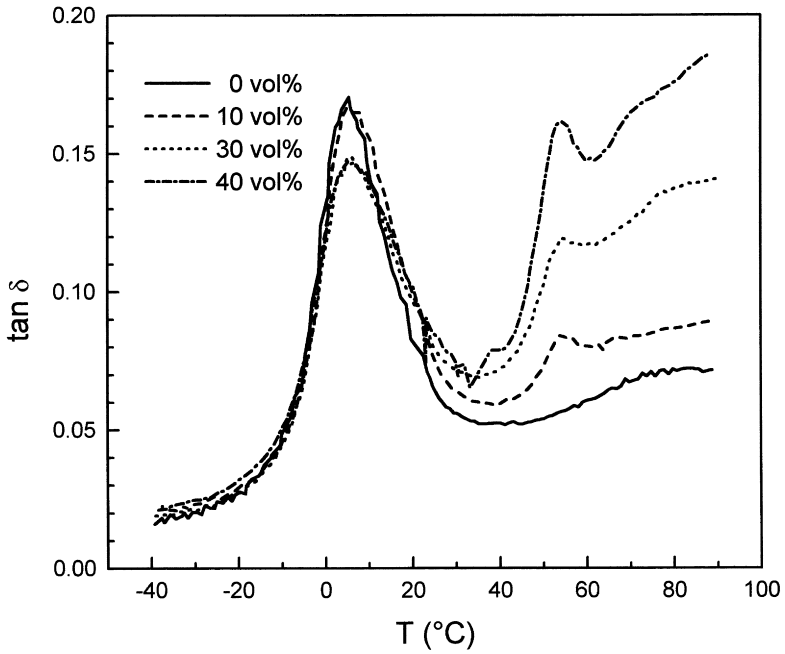

Fig. 2. Influence of temperature on the loss factor tan δ of s-PP containing different glass bead volume fraction ϕ_f.

3. Results and discussion

3.1. Dynamic mechanical properties

Dynamic mechanical properties of filled s-PP were determined as a function of glass bead volume fraction. Fig. 1 shows dynamic storage modulus E' and loss modulus E'' of glass bead filled s-PP as a function of temperature. The dynamic storage modulus characterizes the elastic behaviour, whereas the dynamic loss modulus characterizes the viscous behaviour. As expected, storage modulus decreases with increasing temperature. Both storage modulus E' and loss modulus E'' of the PP composites increase with increasing filler content over the entire temperature range.

Loss modulus E'' of neat s-PP as well as glass bead-filled s-PP have maxima at 0°C. Glass bead-filled s-PP shows an

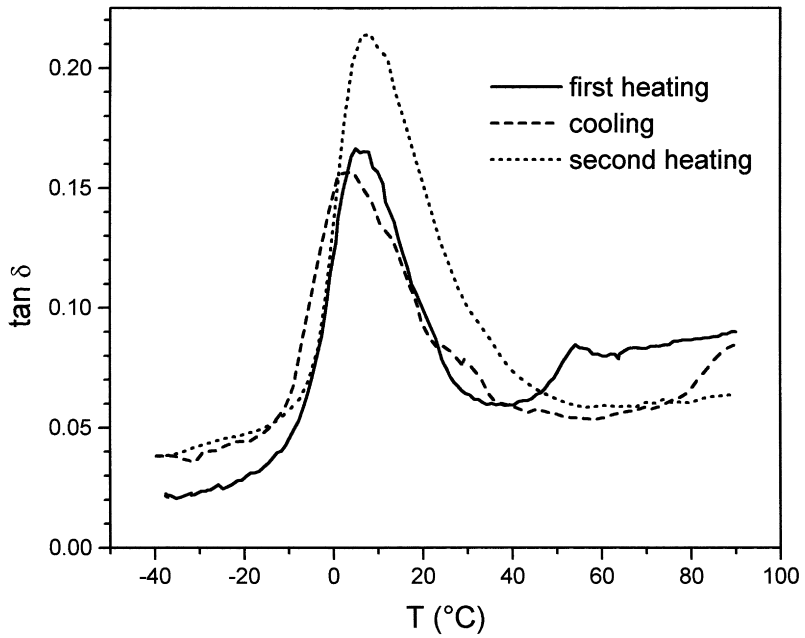

Fig. 3. Loss factor tan δ of s-PP filled with 10 vol% glass beads versus temperature at heating, cooling and second heating process with a heating and cooling rate of 2 K/min.

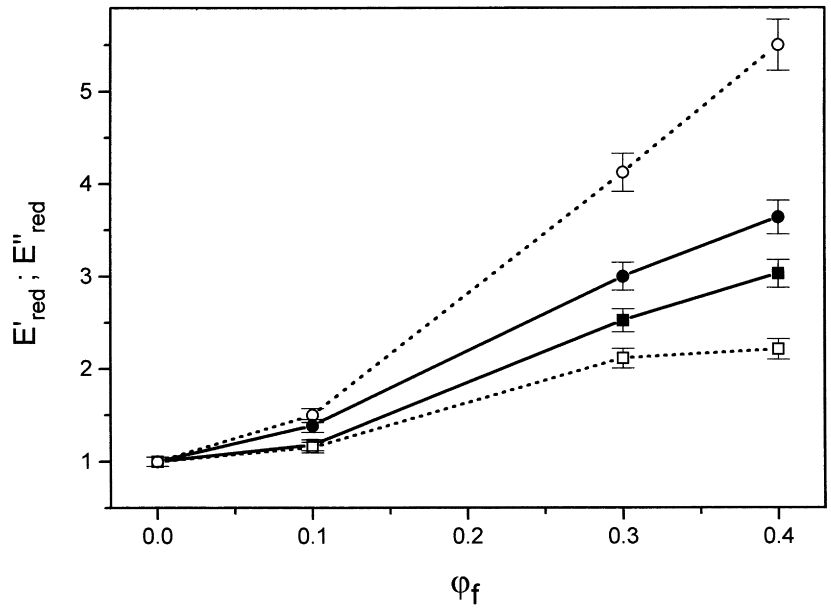

Fig. 4. Reduced storage and loss modulus, E'_{red} (■, □) and E''_{red} (●, ○), of filled s-PP as a function of glass bead volume fraction j_f at 21 (■, ●) and 80°C (□, ○).

additional maximum at 54°C. The plot of dynamic loss factor tan δ *versus* temperature is more sensitive for thermal transitions, as shown in Fig. 2.

The transition at 0°C is caused by the glass transition of s-PP and shows no temperature shift as a function of filler volume fraction, indicating weak interfacial interactions. Strong interfacial interactions should immobilize the s-PP matrix adjacent to the glass surface, effecting a shift of glass transition temperature. The intensity of the maxima decreases with increasing filler loading owing to the reduced s-PP volume fraction. Below 0°C, tan δ is independent of glass bead volume fraction. The second maximum at 54°C cannot be attributed to matrix immobilization at the glass surface, because a shift of more than 50 K is not possible. With increasing glass bead volume fraction the area under the peak is growing and the loss factor above the peak remains at a higher level. Neat s-PP does not show this peak, consequently the glass beads should be responsible for this effect. In Fig. 3, the temperature dependence of the loss factor is illustrated for s-PP filled with 10 vol%

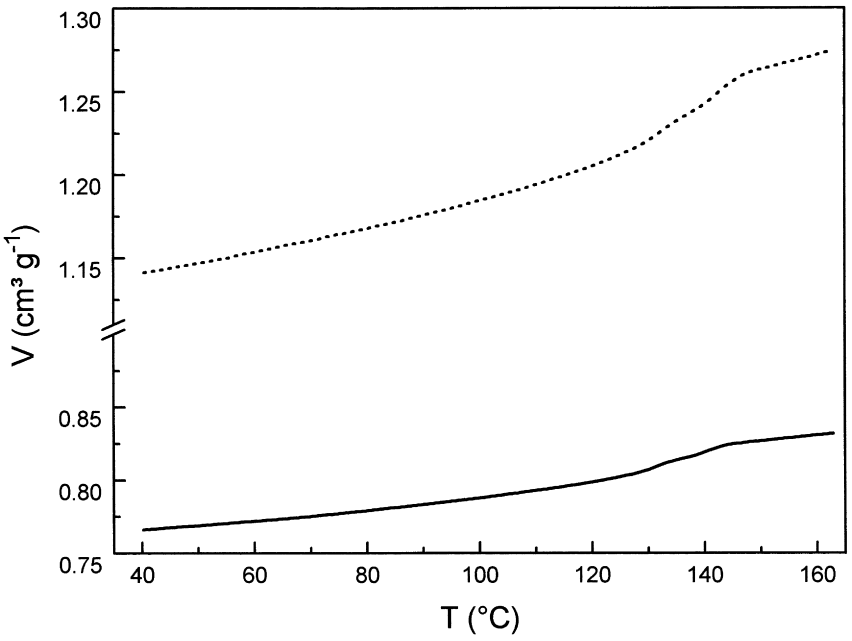

Fig. 5. Isobaric PVT measurements of s-PP (dotted line) and s-PP filled with 30 vol% glass beads (solid line) at 10 MPa.

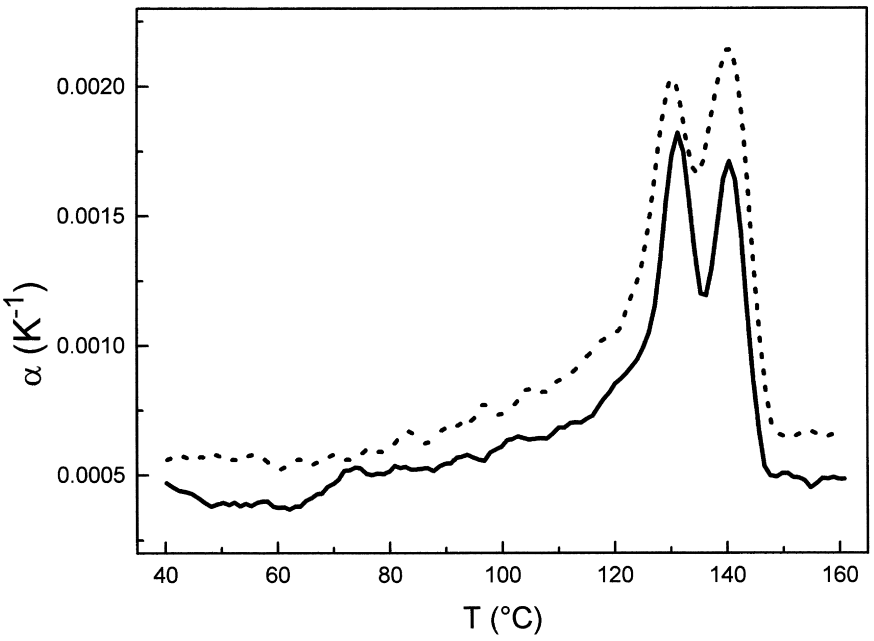

Fig. 6. Temperature dependency of thermal expansion coefficient α of s-PP (dotted line) and s-PP filled with 30 vol% glass beads (solid line) at 10 MPa.

glass beads. The sample was heated up to 90°C, subsequently cooled down to − 40°C and heated up again, all with a heating and cooling rate of 2 K/min. As clearly seen, the peak at 54°C disappears during the cooling and second heating procedure. This indicates that this phase transition is caused by quenching melts of glass bead-filled s-PP, whereas slow cooling and crystallization avoids this effect.

Fig. 4 shows the relative storage and loss modulus (E'_{rel} and E''_{rel}) of glass bead-filled s-PP at 21 and 80°C, given by the ratio of composite and matrix modulus, E'/E'_0 and E''/E''_0, respectively, as a function of glass bead volume fraction. At both temperatures, relative storage and loss modulus increases with increasing glass bead filling. At 80°C the relative storage modulus E'_{rel} of s-PP composites, characterizing the elastic behaviour of the composite, is lower than that at 21°C, owing to the improved molecular mobility of the polymer at elevated temperatures. In contrast, the relative loss modulus E''_{rel} of glass bead-filled s-PP, characterizing the viscous behaviour, increases with increasing temperature.

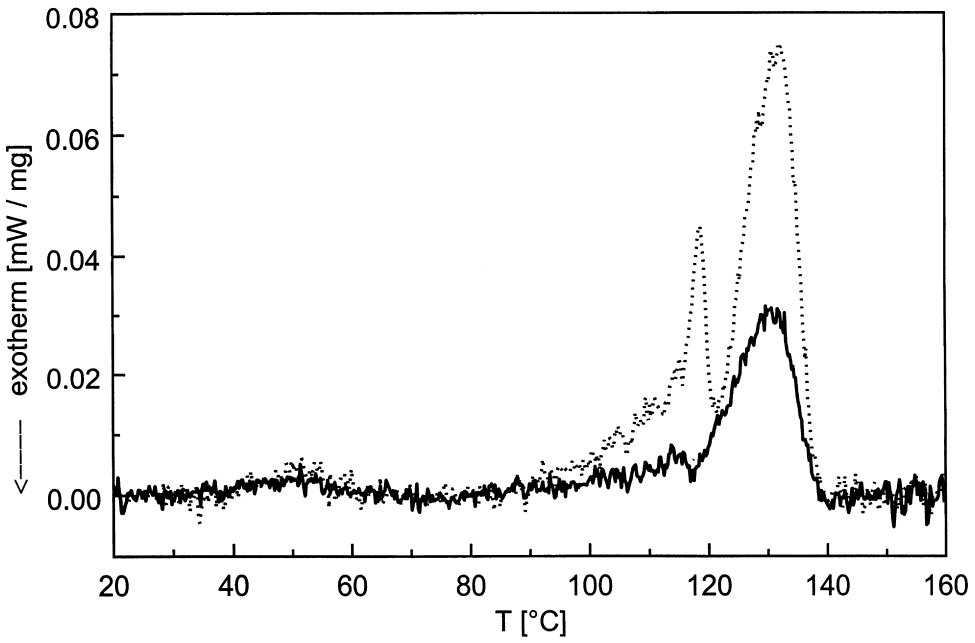

Fig. 7. DSC graphs of s-PP (dotted line) and s-PP containing 30 vol% glass beads (solid line), measured with a heating rate of 2 K/min.

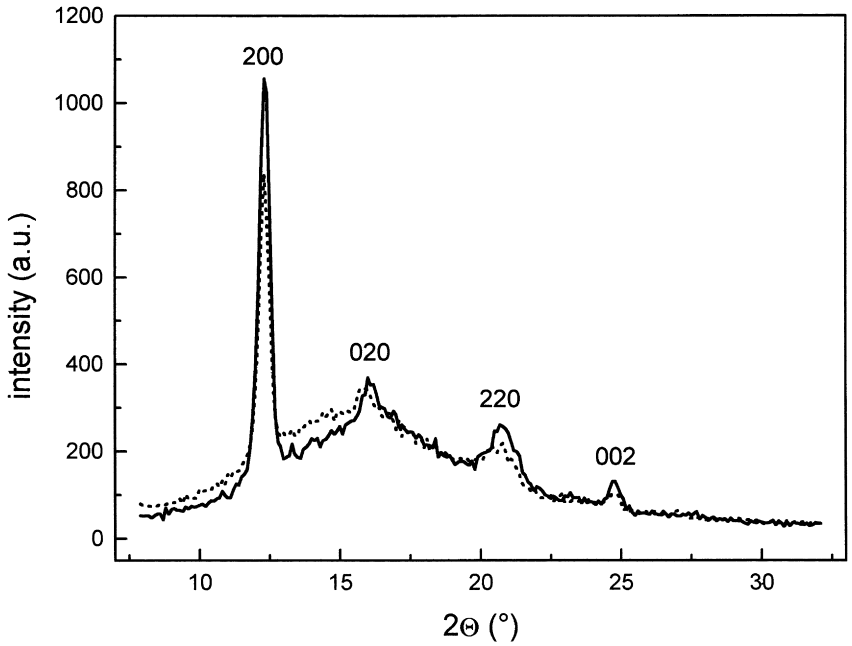

Fig. 8. X-ray powder diffraction patterns of s-PP at 30 (solid line) and 120°C (dotted line).

3.2. PVT and DSC measurements

Fig. 5 shows the isobaric PVT measurements at 10 MPa (100 bar) of s-PP (dotted line) and s-PP filled with 30 vol% glass beads (solid line), respectively. Specific volumes, v_{sp}, of the two samples are shown as a function of temperature between 40 and 180°C. The heating rate was 2 K/min.

The melting temperatures of s-PP and glass bead-filled s-PP between 130 and 140°C are indicated by an inflection point in the corresponding specific volume–temperature curves. Apparently, there is no indication of a phase transition at a lower temperature neither for pure nor for glass bead-filled s-PP. A more sensitive tool for the detection of phase transitions is obtained by plotting the thermal expansion coefficient, α, instead of the specific volume, *versus* temperature. The temperature dependencies of the expansion coefficients of neat (dotted line) and glass bead-filled s-PP (solid line), respectively, are plotted in Fig. 6.

For the neat s-PP as well as for the filled s-PP, two melting transitions can be detected at 131 and 140°C, indicated by two peaks in the corresponding thermal expansion coefficient–temperature curve. This is in accordance with results from Marigo [16], who has observed multiple melting behaviour of s-PP. Within experimental error, no phase transition is detectable for neat s-PP at low temperatures. The situation is different for glass bead-filled s-PP. Here, an increase in α is observed in the temperature range between 60 and 75°C. Assuming a stepwise transition, the transition temperature, given by the inflection point of the step, is located at 68°C. This is significantly higher than the transition temperature observed in DMA measurements. It is well known that with increasing pressure thermal transitions are shifted to higher temperatures [19]. Beside differences arising from employment of different analytical methods this could be an explanation for the differences in transition temperatures obtained by DMA and PVT.

The temperature dependence of the thermal expansion coefficient of a sample is closely related to the temperature dependence of the specific heat, C_p [20], which is monitored by DSC. In Fig. 7, the DSC curves of s-PP (dotted line) and s-PP containing 30 vol% glass beads (solid line) are shown. The corresponding heating rates are 2 K/ min.

Two melting transitions at 130°C and 140°C are visible for both neat and glass bead-filled s-PP. In contrast to the PVT measurements, the melting transition at lower temperature appears much less pronounced compared with the PVT measurements and can hardly be distinguished from the high temperature melting peak. At approximately 55°C, a weak endothermal transition can be detected for both neat as well as for glass bead-filled s-PP. The peak-like shape of the endothermal signals implies that the signal is not caused by a glass transition. The peaks have a similar intensity, but with respect to experimental error are too small to determine transition enthalpies. Because of the reduced s-PP matrix weight fraction in filled s-PP, it can be assumed that the transition enthalpy of filled s-PP is higher than that of neat s-PP.

3.3. WAXS measurements

Fig. 8 shows WAXS patterns of neat s-PP, measured at 30°C (solid line) and 120°C (dotted line). The pattern at 30°C comes from a specimen that was rapidly quenched from the melt after compression molding.

The reflection at $2\Theta = 17°$, typical for the C-centered unit cell type I, is absent [15]. The 020 reflection at $2\Theta = 15.9°$

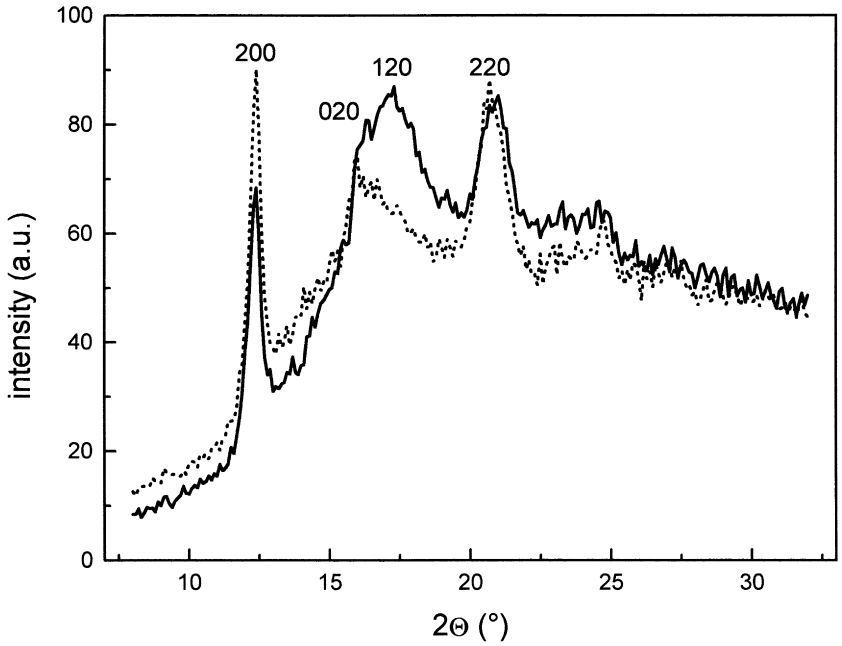

Fig. 9. X-ray powder diffraction patterns of s-PP filled with 30 vol% glass beads at 30 (solid line) and 120°C (dotted line) after compression molding.

and the absence of the 211 reflection at $2\Theta = 18.9°$, which is the primary reflection identifying the unit cell type III, indicates a substantial packing disorder along the *b*-axis, which is typical for packing mode II [3]. Upon heating to 120°C the crystallinity of the sample decreases slightly, but there is no change in modification. Fig. 9 shows WAXS traces of s-PP filled with 30 vol% glass beads, measured at 30°C and 120°C. The thermal history of the sample is similar to neat s-PP, shown in Fig. 8.

The pattern taken at 30°C shows a strong reflection at $2\Theta = 17°$, indicated as 120. As already mentioned, this reflection is typical for the C-centered unit cell type I. Upon heating to 120°C the reflection at $2\Theta = 17°$ disappears and a pattern typical for the unit cell type II results. This behaviour is also known for cell type I crystals in neat s-PP [11]. Fig. 10 shows WAXS patterns of s-PP filled with 30 vol% glass beads measured at 30 and 120°C after passing the tan δ peak of the DMA heating procedure at 55°C.

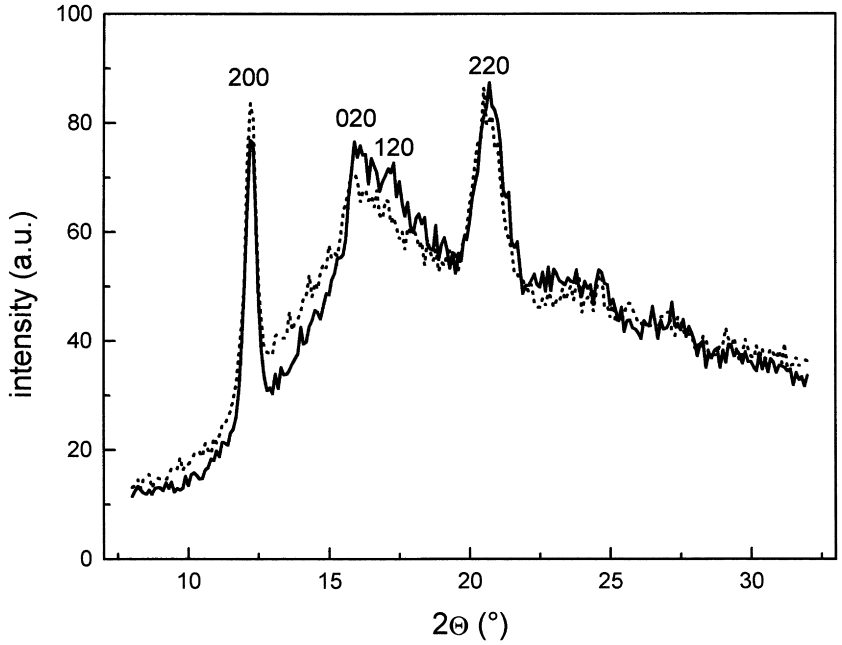

Fig. 10. X-ray powder diffraction patterns of s-PP filled with 30 vol% glass beads at 30 (solid line) and 120°C (dotted line) after passing tan δ peak of the DMA heating procedure at 55°C.

In contrast to Fig. 9 both WAXS traces are typical for a unit cell type II packing mode. The intense peak at $2\Theta = 17°$, present before passing the tan δ peak of the DMA heating procedure (Fig. 9), is absent in both traces. This shows that the tan δ peak at 55°C is related to the disappearance of cell type I crystals.

4. Conclusion

Dynamic mechanical analysis indicates an unexpected thermal transition of glass bead-filled s-PP at 54°C. The signal intensity increases with increasing glass bead volume fraction and is not observed for neat s-PP. PVT measurements at a pressure of 10 MPa show a thermal transition at 68°C, which is attributed to the DMA signal at 54°C. The high pressure employed in the PVT measurements (10 MPa, compared with atmospheric pressure in DMA measurements) is possibly responsible for the differences encountered in the transition temperatures. The transition can also be detected by DSC (55°C), although the intensities of the signals are too weak for quantitative analysis. Nevertheless, neat s-PP also shows such a signal, whereas DMA and PVT analysis do not reveal a corresponding peak at this temperature. In consideration of filler loading, the DSC signal of neat s-PP is smaller than that of glass bead-filled s-PP. DMA and DSC indicate that the thermal transition cannot be attributed to polymer immobilization at the glass surface, effecting changes in glass transition temperature. WAXS measurements show that at experimental conditions neat s-PP crystallizes in a modification of unit cell type II. Glass bead-filled s-PP, prepared under identical experimental conditions, crystallizes in a modification of unit cell types I and II, which converts to unit cell type II at approx. 54°C. This conversion was detected by DMA, DSC and PVT. Furthermore, a glass transition temperature of s-PP (0°C) can be detected by DMA, as well as melting behaviour by DSC and PVT. Both methods reveal the multiple melting behaviour of s-PP, which can be attributed to a melting–recrystallization process.

Acknowledgements

The authors would like to thank Shell Research Centre in Louvain-la-Neuve, Belgium, for supporting this study.

References

[1] Thomann R, Wang C, Kressler J, Jüngling S, Mülhaupt R. Polymer 1995;36(20):3795.
[2] Rodriguez-Arnold J, Zhang A, Cheng SZD, Lovinger AJ, Hsieh ET, Chu P, Johnson TW, Honnell KG, Geerts RG, Palackal SJ, Hawley GR, Welch MB. Polymer 1884;1994:35.
[3] Lovinger AJ, Lotz B, Davis DD, Schumacher M. Macromolecules 1994;27:6603.
[4] Stocker W, Schumacher M, Graff S, Lang J, Wittmann JC, Lovinger AJ, Lotz B. Macromolecules 1994;27:6948.
[5] Moore EP. Polypropylene handbook. Munich: Hanser, 1996.
[6] Lotz B, Wittmann JC, Lovinger AJ. Polymer 1996;37(22):4979.
[7] Ewen JA, Jones RL, Razavi A, Ferrara JD. J Am Chem Sci 1988;110:6255.
[8] Natta G, Corradini P, Ganis P. J Polym Sci 1962;58:1191.
[9] Natta G, Peraldo M, Allegra G. Makromol Chem 1964;75:215.
[10] Chatani Y, Maruyama H, Noguchi K, Asanuma T, Shiomura T. J Polym Sci Part C: Polym Lett 1990;28:393.
[11] Loos J, Hückert A, Petermann J. Colloid Polym Sci 1996;274:1006.
[12] Chatani Y, Maruyama H, Asanuma T, Shiomura T. J Polym Sci Part B: Polym Phys 1991;29:1649.
[13] Corradini P, Natta G, Ganis P, Temussi PA. J Polym Sci Part C 1967;16:247.
[14] Lotz B, Lovinger AJ, Cais RE. Macromolecules 1988;21:2375.
[15] De Rosa C, Corradini P. Macromolecules 1993;26:5711.
[16] Marigo A, Marega C, Zannetti R. Macromol Rapid Commun 1994;15:225.
[17] Stricker F, Bruch M, Mülhaupt R. Polymer 1997;38:5347.
[18] Zoller P, Bolli P, Pahud V, Ackerman H. Rev Sci Instrum 1976;49:948.
[19] Skorodumov VF, Godovskii YK. Polym Sci 1993;35:214.
[20] Landau LD, Lachieser A, Lifschitz EM. Mechanik und molekularphysik. Berlin: Akademie, 1970.